

In Situ SAXS Studies of the Structural Changes of Polymer Nanocomposites Used in Battery Applications

Giselle Sandí,^{*,†} Humberto Joachin,[‡] Riza Kizilel,[‡] Sönke Seifert,[†] and Kathleen A. Carrado[†]

Chemistry Division, Argonne National Laboratory, 9700 South Cass Avenue, Argonne, Illinois 60439-4803, and Department of Chemical and Environmental Engineering, Illinois Institute of Technology, 10 W. 33rd Street, Chicago, Illinois 60616

Received June 14, 2002. Revised Manuscript Received November 21, 2002

In situ small-angle X-ray scattering studies have been conducted to monitor the structural changes of polymer nanocomposites upon heating. These nanocomposites are made of different mass ratios of poly(ethylene oxide) and synthetic lithium hectorite. The samples were heated under nitrogen to avoid oxidation of the organic matrix. On the basis of the in situ results, it was found that the polymer matrix loses its crystallinity at about 60 °C and the composite is stable up to 150 °C.

Introduction

The modification of polymer properties by the addition of another material, that is, a filler, have been studied for many years. Common fillers such as glass fibers, carbon fibers and carbon black, pigments, and minerals, including silicates, are used to modify the macroscopic properties of the polymer, such as modulus and toughness.^{1–3} In recent years, a new class of materials have been developed by dispersing layered silicates with polymers at the nanoscale level. These new materials have attracted wide interest because they often exhibit chemical and physical characteristics that are very different from the starting material.^{4,5} In some cases, the silicates and polymers exist as alternating layers of inorganic and organic.^{6–8} The possibility of improved mechanical, rheological, electrical, and optical properties and the ability to exercise control over existing physical and chemical behavior have led to a large number of studies of these materials, including composites of layer silicate clays with poly(ethylene oxide) (PEO),^{9–11} epoxy resin,^{12–14} polystyrene,^{15,16} and a range of other thermoplastics and elastomers.^{17–20}

It is known that polymer electrolytes exhibit high conductivity only in the absence of a crystalline phase,¹⁰ which impedes the transport of ions, and only at temperatures well above the glass-transition temperature (T_g). A number of methods have been used to prepare totally amorphous polymers of high conductivity, including random copolymers²¹ or branched block copolymers.²² However, the mechanical strength of these polymers is often poor because of their low transition temperatures. Mechanical strength can be maintained by cross-linking of the polymer chains, but this comes at the expense of reduced conductivity. Another approach to increasing conductivity is to incorporate low molecular weight plasticizers into the polymer.²³ A large amount of effort has gone into understanding the interactions of the plasticizers with the polymer chain and also the ionic species.

Nanocomposite materials of PEO and phyllosilicates were first suggested by Ruiz-Hitzky and Aranda¹ as candidates for polymer electrolytes. Within these materials, the polymer chains are intercalated between the silicate layers. The polymer chains then provide a mobile matrix in which cations are able to move. A considerable amount of interest has been shown in nanocomposites of PEO and montmorillonite,^{1–3,6–11} a

* To whom correspondence should be addressed. Phone: 630-252-1903. Fax: 630-252-9288. E-mail: gsandi@anl.gov.

[†] Argonne National Laboratory.

[‡] Illinois Institute of Technology.

(1) Ruiz-Hitzky, E.; Aranda, P. *Adv. Mater.* **1990**, *2*, 545.

(2) Aranda, P.; Ruiz-Hitzky, E. *Chem. Mater.* **1992**, *4*, 1395.

(3) Vaia, R. A.; Ishii, H.; Giannelis, E. P. *Chem. Mater.* **1993**, *5*, 1694.

(4) *Polymer-Clay Nanocomposites*; Beall, G., Pinnavaia, T. P., Eds.; Wiley & Sons: Chichester, U.K., 2000.

(5) Carrado, K. A. In *Advanced Polymeric Materials: Structure Property Relationships*; Advani, S. G., Shonaike, G. O., Eds.; Technomic Publ.: Lancaster, PA, 2002; in press.

(6) Lemmon, J. P.; Wu, J.; Oriakhi, C.; Lerner, M. *Electrochim. Acta* **1995**, *40*, 2245.

(7) Vaia, R. A.; Jandt, K. D.; Kramer, E. J.; Giannelis, E. P. *Macromolecules* **1995**, *28*, 8080.

(8) Tunney, J. J.; Detellier, C. *Chem. Mater.* **1996**, *8*, 927.

(9) Mehrotra, V.; Giannelis, E. P. *Mater. Res. Soc. Symp. Proc. (Polymer Based Molecular Composites)* **1990**, *171*, 39.

(10) Vaia, R. A.; Sauer, B. B.; Tse, O. K.; Giannelis, E. P.; *J. Polym. Sci., Part B: Polym. Phys.* **1997**, *35*, 59.

(11) Wong, S.; Vaia, R. A.; Giannelis, E. P.; ZAX, D. B. *Solid State Ionics* **1996**, *86–88*, 547.

(12) Wang, M. S.; Pinnavaia, T. J. *Chem. Mater.* **1994**, *6*, 468.

(13) Lee, D. C.; Jang, L. W. *J. Appl. Polym. Sci.* **1998**, *68*, 1997.

(14) Lan, T.; Kaviratna, D.; Pinnavaia, T. J. *J. Phys. Chem. Solids* **1996**, *57*, 1005.

(15) Moet, A. S.; Akelah, A. *Mater. Lett.* **1993**, *18*, 97.

(16) Porter, T. L.; Hagerman, M. E.; Reynolds, B. P.; Eastman, M. P.; Partnell, R. A. *J. Polym. Sci., Part B: Polym. Phys.* **1998**, *36*, 673.

(17) Reichert, P.; Kressler, J.; Thomann, R.; Mulhaupt, R.; Stopelmann, G. *Acta Polym.* **1998**, *56*, 116.

(18) Biswas, M.; Ray, S. S. *Polymer* **1998**, *39*, 6423.

(19) Ramachandran, K.; Lerner, M. M. *J. Electrochem. Soc.* **1997**, *144*, 3739.

(20) Wang, Z.; Pinnavaia, T. J. *Chem. Mater.* **1998**, *10*, 3769.

(21) Nicholas, C. V.; Wilson, D. J.; Booth, C.; Giles, J. R. *Br. Polym. J.* **1988**, *20*, 289.

(22) Blonsky, P. M.; Shiver, D. F.; Austin, P.; Allcock, H. R. *J. Am. Chem. Soc.* **1984**, *106*, 6854.

(23) Andrieu, X.; Vicedo, T.; Fringant, C. *J. Power Sources* **1995**, *54*, 487.

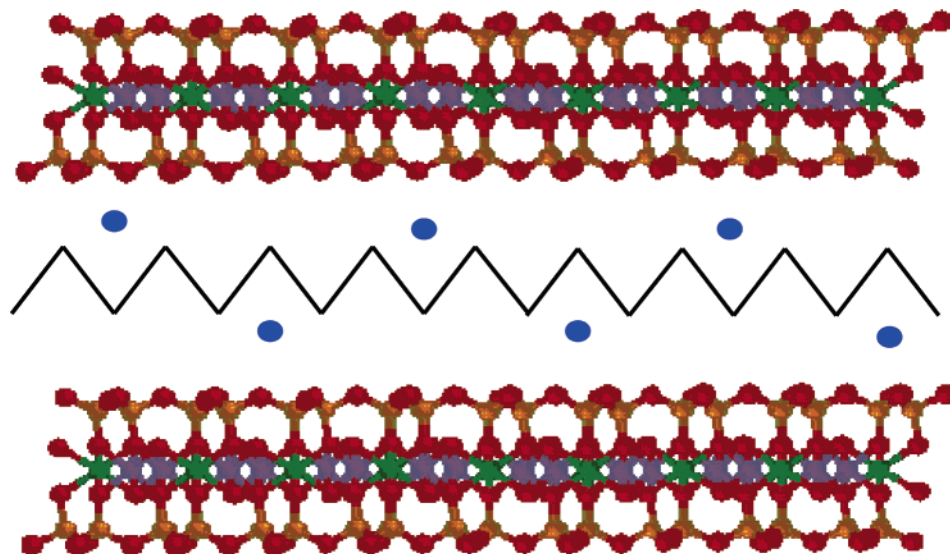


Figure 1. Schematic representation of lithium hectorite clay. The gallery region shows one PEO layer and exchangeable Li(I) cations.

layered aluminosilicate clay. When this composite contains LiBF_4 , it displays conductivities up to 2 orders of magnitude larger than that of PEO itself at ambient temperatures.¹¹ However, the addition of lithium salts, which is needed to obtain such conductivity values, is not desirable for two reasons; the first one relates to a more complicated synthetic route and the second relates to the fact that transference numbers are not unity since in this case both cations and anions move.

We have prepared a series of nanocomposites containing PEO intercalated in the layers of hectorite clays. These clays, also called phyllosilicates, belong to the family of smectite clay minerals. They are composed of two tetrahedral silicate layers sandwiching a central octahedral layer in a so-called 2:1 arrangement. In hectorite, isomorphous substitutions in the lattice of Li(I) for Mg(II) in the octahedral layers cause an overall negative charge that is compensated by the presence of interlayer, or gallery, cations. A significant amount of interlayer water is also present and the cations are easily exchangeable. A large degree of preferential orientation in films prepared by naturally occurring clays tends to occur, however, due to their large platelet size (up to 1 mm). This can lead to nonconducting planes being perpendicular to the current path and thus reduce the conductivity. To avoid this problem, we followed a method developed by Carrado et al.,²⁴ which involves direct hydrothermal synthesis and crystallization of hectorite with smaller platelet size, termed synthetic lithium hectorite (SLH). Organic molecules can be incorporated either directly from the gel or by subsequent intercalation. Figure 1 shows a schematic structure of intercalated PEO in a SLH. The circles in the gallery represent Li ions.

There has been a considerable amount of work performed by Giannelis and co-workers^{7,10,11} related to the synthesis of nanocomposite films derived from PEO and montmorillonite using a melt intercalation procedure. Doeffer and Reed²⁵ have reported the formation of

PEO/Laponite (a commercially available synthetic hectorite) electrolytes; however, their conductivity is low. To the best of our knowledge, PEO/SLH nanocomposites have not been used as polymer electrolytes. The aims of this paper are to study in situ the structural changes of PEO/SLH nanocomposites as a function of temperature, to establish the temperature at which PEO loses its crystallinity in this matrix, and to correlate these parameters with conductivity.

Experimental Section

Preparation of the SLH clay via hydrothermal crystallization at 100 °C of silica sol, magnesium hydroxide, and lithium fluoride can be found in detail in ref 24. In brief, precursor clay gels are of the composition $1.32:5.3:8:n \text{ LiF:Mg(OH)}_2\text{:SiO}_2\text{:H}_2\text{O}$ to correlate with the ideal hectorite composition of $\text{Li}_{0.66}[\text{Li}_{0.66}\text{Mg}_{5.34}\text{Si}_8\text{O}_{20}(\text{OH},\text{F})_4]$. A typical reaction begins by suspending the LiF with stirring in water. Separately, $\text{MgCl}_2 \cdot 6\text{H}_2\text{O}$ is dissolved in water and mixed with 2 N NH_4OH to crystallize fresh Mg(OH)_2 . Prior to use, this brucite source must be washed several times with water to remove excess ions. It is then added wet to the LiF solution. This slurry is stirred for 15–30 min before addition of silica sol (Ludox HS-30, Na^+ -stabilized, 30%). The total volume is increased to afford a 2 wt % solids suspension and is stirred and refluxed for 40–48 h. Solids are isolated by centrifugation, washed, and air-dried.

Colloidal suspensions of 1 g of SLH/100 mL of deionized water were stirred for 0.5 h. The desired amount of PEO (100 000 average molecular weight, from Aldrich) was then added and the mixture stirred for 24 h. Mixtures contained 0.6, 0.8, 1.0, and 1.2 g of PEO/g of clay. Films were prepared by puddle-casting the slurries onto Teflon-coated glass plates and air-drying. Further drying was carried out at 120 °C under an inert atmosphere for at least 48 h. The typical thickness of the films is about 40 μm . For comparative purposes, films of PEO/Laponite were prepared as per ref 25.

X-ray powder diffraction (XRD) patterns of SLH and PEO powders were determined using a Rigaku Miniflex, with $\text{Cu K}\alpha$ radiation and a NaI detector at a scan rate of 0.5° $2\theta/\text{min}$ and step size of 0.05.

In situ small-angle X-ray scattering (SAXS) was carried out at the Advanced Photon Source (Basic Energy Sciences Synchrotron Research Center CAT), Argonne National Laboratory. The SAXS intensity of the investigated material $I(q)$ is the function of the angle of scattering (2θ) and the wave-

(24) (a) Carrado, K. A.; Winans, R. E.; Botto, R. E. U.S. Patent 5,308,808. (b) Carrado, K. A. *Appl. Clay Sci.* **2000**, *17*, 1.

(25) Doeffer, M.; Reed, J. S. *Solid State Ionics* **1998**, *113–115*, 109.

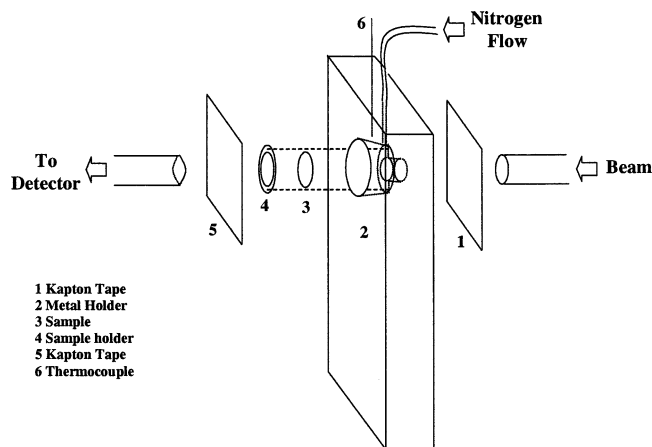


Figure 2. Schematic diagram of the sample holder used for in situ SAXS studies.

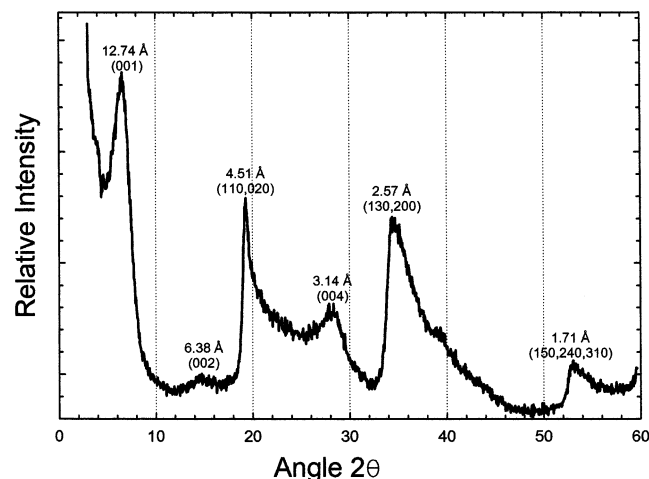


Figure 3. X-ray powder diffraction pattern of SLH. The inset shows the major diffraction peaks.

length (λ) of the applied radiation. This relation can be expressed as $q = 4\pi \sin \theta / \lambda$. Monochromatic X-rays (18 keV) are scattered off the sample and collected on a 15×15 cm² CCD camera. The scattered intensity is corrected for absorption and instrument background. The differential scattering cross section is expressed as a function of the scattering vector q . The value of q is proportional to the inverse of the length scale (\AA^{-1}). The instrument was operated with a sample-to-detector distance of 332 mm to obtain data at $0.1 < q < 3.0$ \AA^{-1} . For these studies, a specially designed sample holder was used to heat up the sample and collect SAXS data at the same time. Figure 2 shows a diagram of the sample holder. Films of about 1.25 cm in diameter and 40 μm in thickness were placed in the sample holder and held using Kapton tape. The furnace temperature program was set to ramp from room temperature to 150 °C at 5 °C/min, and the gas flow of nitrogen was started at room temperature. Temperature readings have an error of ± 5 °C. SAXS data were collected at room temperature and 60, 80, 100, 120, and 150 °C to compare the structural results with the conductivity values. The sample holder with a piece of Kapton tape heated at each temperature was used as the blank and all the SAXS data were corrected accordingly.

ac impedance measurements as a function of temperature were obtained on films in sealed cells with lithium foil as the counter and working electrode, using a Solartron SI 1256 electrochemical interface and 1254 frequency response analyzer. A Tenney Junior Environmental Test Chamber was used to controlled the temperature of the cell with a precision of ± 0.5 °C.

Transmission electron microscopy (TEM) was performed in a JEOL 100CXII transmission electron microscope operating

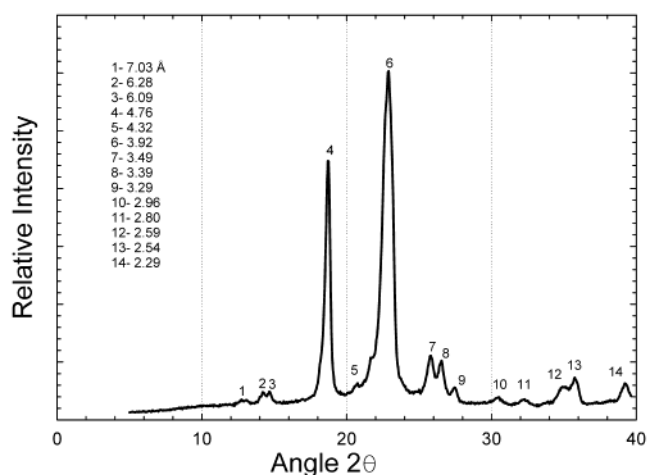


Figure 4. X-ray powder diffraction pattern of PEO. The inset shows the major diffraction peaks.

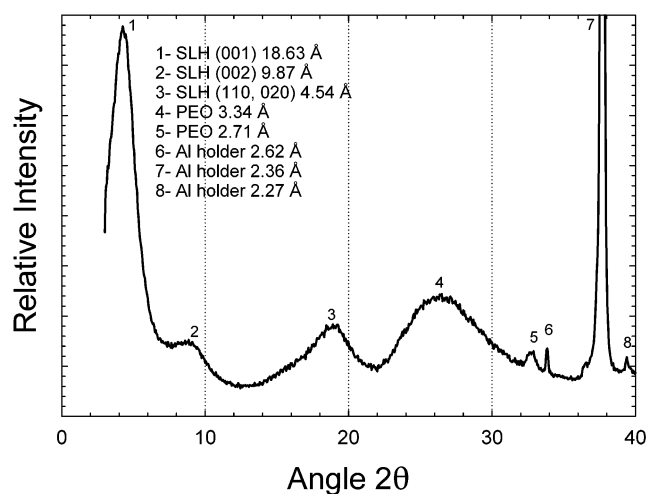


Figure 5. X-ray powder diffraction pattern of a film containing a PEO/SLH 1:1 ratio. The inset shows the major diffraction peaks.

at 100 kV. Approximately 0.2 mL of a 1:1 PEO/SLH slurry was placed into a vial and sonicated for 30 s. Copper grids were then dipped into the resulting slurry. The Cu grids were allowed to dry for 2 h in a vacuum oven at 100 °C. Once dry, the grids were inserted into nontilt holders and loaded into the instrument. Scale markers placed on the micrographs are accurate to within 3%.

Results and Discussion

Understanding the structural changes of the PEO component in the nanocomposite films upon heating is crucial for predicting the conductivity of these materials. In situ SAXS is an excellent technique for deriving such information because of this particular instrument's time-resolving capability and its high flux.

For comparison with SAXS data, X-ray powder diffraction of SLH and PEO powders were obtained. Figure 3 shows the X-ray powder diffraction of the SLH powder. The peaks are indexed as indicated on the graph. The distance between clay sheets is given by the d_{001} reflection and corresponds to 12.7 Å, which includes one clay lattice unit at 9.6 Å. The gallery region therefore corresponds to 3.1 Å and contains Li(I) cations and water in this case. Because smectites are capable of swelling, this region can easily accommodate one or

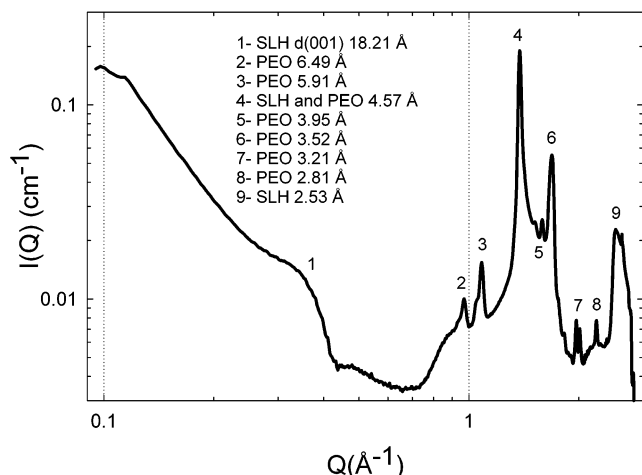


Figure 6. In situ SAXS of a PEO/SLH 1.2:1 mass ratio film taken at room temperature. The inset shows the diffraction peaks attributed to PEO and SLH.

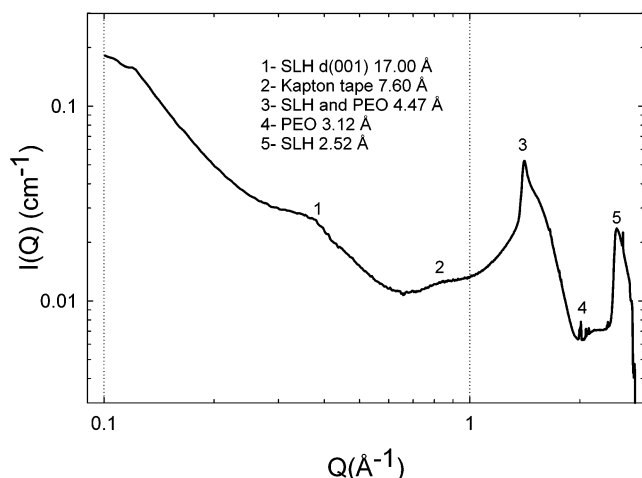


Figure 7. In situ SAXS of a PEO/SLH 1.2:1 mass ratio film taken at 60 °C. The sharp peaks from PEO have broadened, indicating that the PEO has lost its crystallinity. The sample was heated under nitrogen at 5 °C/min.

more layers of PEO.² Figure 4 shows the diffraction pattern of the PEO powder used to make the films. The peaks are quite sharp, which indicates the crystalline nature of the starting material. An XRD pattern of a film containing PEO/SLH 1:1 ratio is shown in Figure 5. The d_{001} reflection has increased by 5.89 Å, indicating that the PEO has been intercalated within the clay galleries.

Figure 6 shows SAXS data obtained from a film made of PEO/SLH 1.2:1 mass ratio. The data were collected at room temperature. This figure was chosen because it shows clearly the peaks that correspond to SLH and PEO. The d_{001} peak is broader than that presented in the XRD plots (because it is plotted here as Q in \AA^{-1}), but the spacing differs only by 0.42 Å. SAXS data were then collected at 60 °C and the results are shown in Figure 7. It is clear that the structure of the polymer has changed as indicated by the near complete disappearance of the PEO crystalline peaks. It is therefore assumed that the polymer chains have relaxed inside the clay layers. Other evidence of such relaxation is the decrease in d_{001} spacing, which indicates a more dense polymer phase. Under these circumstances, the polymer matrix is more mobile and the lithium ions associated

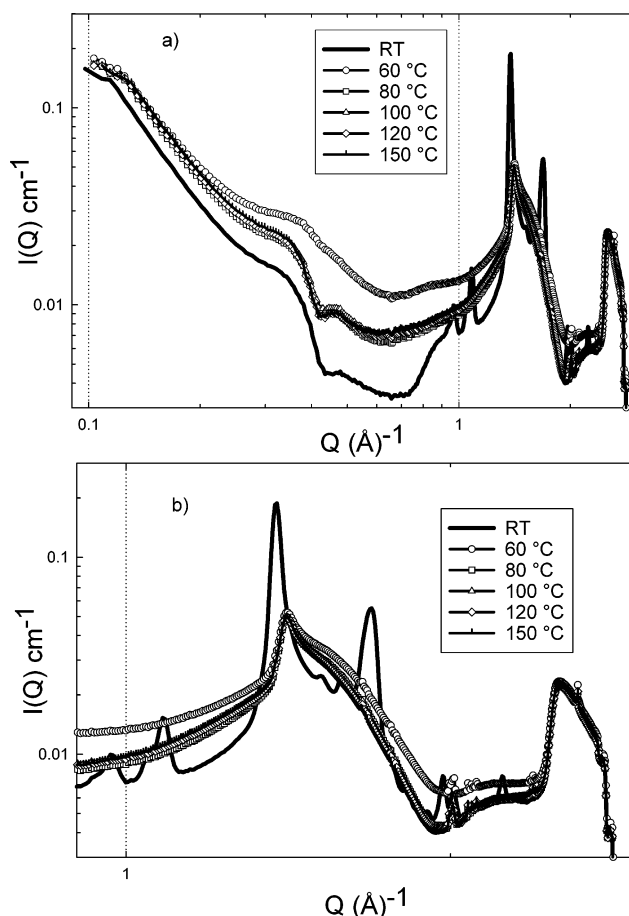


Figure 8. (a) In situ SAXS of a PEO/SLH 1.2:1 mass ratio film taken at 60, 80, 100, 120, and 150 °C. The sharp peaks from PEO have broadened, indicating that the PEO has lost its crystallinity. The sample was heated under nitrogen at 5 °C/min. (b) Same as (a), but with the x -axis expanded.

with the polymer can have higher transference number, leading to a higher conductivity as found by Sandí et al.²⁶ The samples were also heated at 80, 100, 120, and 150 °C and the results are shown in Figure 8a,b. Except for complete disappearance of the PEO peaks at 80 °C, there are no other polymer structural changes. Due to the PEO content of these nanocomposites, it is possible that part of the polymer remains adsorbed at the clay surface and that, after heating of the samples, this PEO can re-intercalate. After the samples were heated at 150 °C, they were cooled at room temperature and a SAXS measurement was performed. The results suggested that the loss of PEO crystallinity is irreversible; that is, no crystalline peaks were observed. Therefore, no evidence for an additional intercalation process was observed, contrary to what others have observed.^{27,28}

The conductivity of the nanocomposite was determined at the same temperature as the SAXS in situ data to correlate the changes in the nanocomposite structure with conductivity. Figure 9 shows a plot of

(26) Sandí, G.; Carrado, K. A.; Joachin, H.; Lu, W.; Prakash, J. Submitted to *J. Power Sources*, **2002**.

(27) Vaia, R. A.; Vasudevan, S.; Krawiec, W.; Scanlon, L. G.; Giannelis, E. P. *Adv. Mater.* **1995**, 7, 154.

(28) Aranda, P.; Galván, J. C.; Ruiz-Hitzky, E. In *Organic/Inorganic Hybrid Materials*; Laine, R. M., Sánchez, C., Brinker, C. J., Giannelis, E., Eds.; MRS Symposium Proceedings 519; Materials Research Society: Warrendale, PA, 1998; p 375.

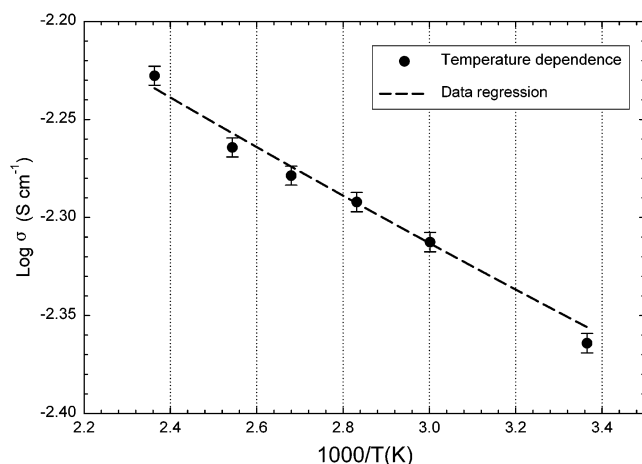


Figure 9. Conductivity as a function of temperature of the nanocomposite with nominal composition PEO/SLH 1:1 mass ratio.

Table 1. Transference Numbers Obtained for Different PEO/SLH Mass Ratios as a Function of Temperature

composition PEO/SLH	temperature					
	RT	60 °C	80 °C	100 °C	120 °C	150 °C
0.6:1	0.88	0.92	0.92	0.93	0.93	0.93
0.8:1	0.90	0.95	0.95	0.95	0.94	0.94
1:1	0.87	0.91	0.92	0.93	0.93	0.93
1.2:1	0.87	0.90	0.90	0.91	0.91	0.92

conductivity as a function of temperature of the nanocomposite with nominal composition PEO/SLH 1:1 mass ratio. As found by Riley et al.²⁹ and Chen et al.,³⁰ the conductivity of the polymer nanocomposites increases as the sample is heated from room temperature (26.0 °C) to 150 °C. As shown in the plot, the largest increase in conductivity occurs between room temperature and 60 °C, in accordance with the decrease on the polymer crystallinity. Similar behavior was observed for the PEO/SLH 0.6:1, 0.8:1, and 1.2:1 samples.

Transference numbers were obtained following the procedures outlined by Dees et al.³¹ As anticipated for a single-ion conductor, the transference numbers obtained as a function of temperature were very close to unity (Table 1). Same as with the conductivity values, the largest increase in the numbers is observed from room temperature to 60 °C, in accordance with the conductivity values and the loss of polymer's crystallinity.

In situ studies were also performed on the nanocomposites samples with ratios of 0.6, 0.8, and 1.0 g of PEO/g of clay. The results of the 0.8 g of PEO/SLH are shown in Figure 10. The changes are identical to the other films (results of the 1:1 and 0.6 not shown). The only difference resides in the intensity of the PEO peak at 4.47 Å, which decreases slightly as the amount of PEO in the film decreases.

For comparative purposes, in situ SAXS studies were also performed on films made with PEO/Laponite at different mass ratios. Figure 11 shows the data taken

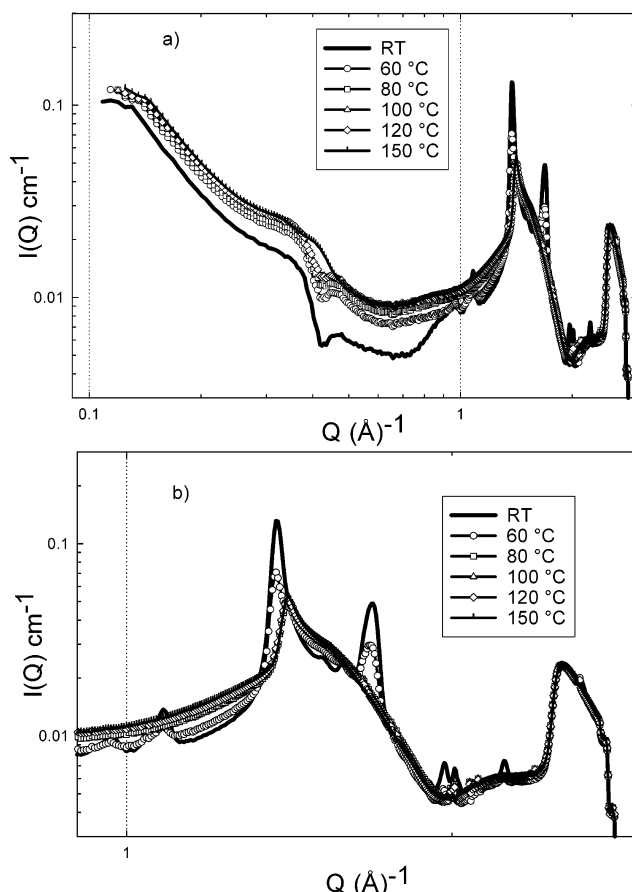


Figure 10. (a) In situ SAXS of a PEO/SLH 0.8:1 mass ratio film taken at 60, 80, 100, 120, and 150 °C. The sharp peaks from PEO have broadened, indicating that the PEO has lost its crystallinity. The sample was heated under nitrogen at 5 °C/min. (b) Same as (a), but with the x -axis expanded.

at different temperatures of a film made with a mass ratio of PEO/Laponite of 1.2:1. The data are similar to the PEO/SLH; however, the conductivity of the PEO/SLH films is at least 1 order of magnitude higher (at 60 °C) than the films made of PEO/Laponite.²⁵ The SLH has larger particle size than Laponite³² and about 20% silica impurity³³ and either of which may be responsible for the higher conductivity. Figure 12 shows the TEM of a 1:1 PEO/SLH membrane, wherein small 20-nm disks due to silica spheres are visible throughout the background. Croce et al.³⁴ demonstrated that with dispersion of selected low-particle size ceramic powders (γ -LiAlO or TiO₂) in PEO-LiX polymer electrolytes nanocomposites, enhanced interfacial stability as well as improved conductivity at ambient temperature were achieved. Commercially available Laponite such as that used by Doeff and Reed²⁵ does not contain silica particles. As discussed by Mermut and Cano,³⁵ other clay materials such as those recently used by Giannelis and co-workers,³⁶ contain negligible amounts of silica

(29) Riley, M.; Fedkiw, P. S.; Khan, S. A. *J. Electrochem. Soc.* **2002**, *149* (6), A667.

(30) Chen, H. W.; Chiu, C. Y.; Chang, F. C. *J. Polym. Sci., Part B: Polym. Phys.* **2002**, *40*, 1342.

(31) Dees, D. W.; Battaglia, V. S.; Redey, L.; Henriksen, G. L.; Atanasoski, R.; Bélanger, A. *J. Power Sources* **2000**, *89*, 249.

(32) Carrado, K. A.; Csencsits, R.; Thiagarajan, P.; Seifert, S.; Macha, S. M.; Harwood, J. S.; Kizilel, R. *J. Mater. Chem.* **2002**, in press.

(33) Carrado, K. A.; Xu, L.; Gregory, D.; Song, K.; Seifert, S.; Botto, R. *Chem. Mater.* **2000**, *12*, 3052.

(34) Croce, F.; Appetecchi, G. B.; Persi, L.; Scrosati, B. *Nature* **1998**, *394*, 456.

(35) Mermut, A. R.; Cano, A. F. *Clays Clay Miner.* **2001**, *49* (5), 381.

(36) Hackett, E.; Manias, E.; Giannelis, E. P. *Chem. Mater.* **2000**, *12*, 2161.

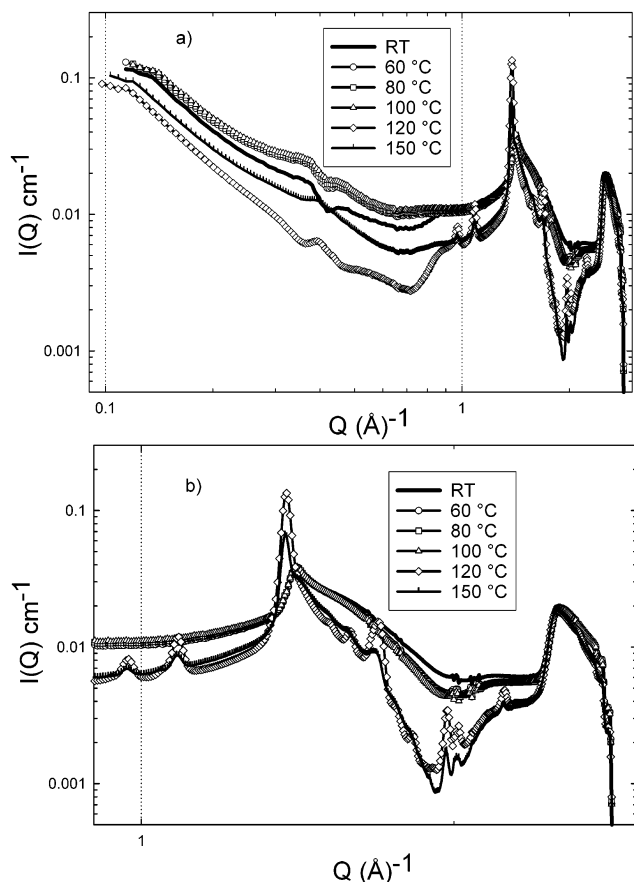


Figure 11. (a) In situ SAXS of a PEO/Laponite 1.2:1 mass ratio film taken at 60, 80, 100, 120, and 150 °C. The pattern is almost identical to that of the PEO/SLH film. The sharp peaks from PEO broadened when the film was heated to 60 °C, indicating that the PEO lost its crystallinity. The sample was heated under nitrogen at 5 °C/min. (b) Same as (a), but with the x -axis expanded.

impurities. For example, when Li-fluorohectorite is made by a high-temperature solid-state melting process, it does not contain any silica. SAZ-1 montmorillonite has at most only about 1% quartz and similarly small amounts of cristobalite or opal as the only silica impurities. Swy-2 is about 95% clay when purified and 4% of the impurities are quartz. Most montmorillonites are fairly pure and do not have much silica. Our synthetic route leads to the production of polymeric nanocomposites with enhanced conductivity without addition of ceramic or oxide fillers.

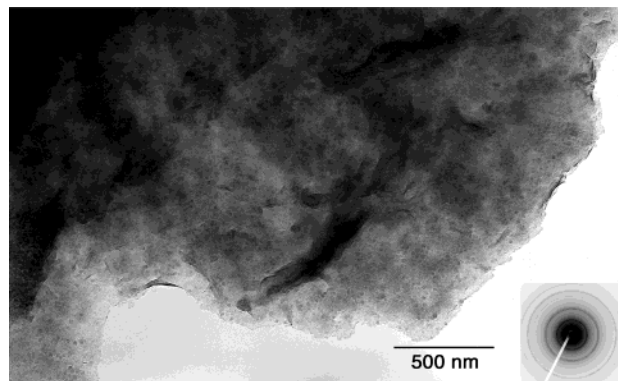


Figure 12. TEM of a 1:1 PEO/SLH mass ratio nanocomposite membrane. Silica spheres (20-nm disks) are visible throughout the background.

Conclusions

In situ SAXS studies show that the structural changes, as a function of temperature, of polymer nanocomposites derived from PEO/SLH can be obtained with detail. At 60 °C, PEO loses its crystallinity and it is at this point where the films become more conductive, as also indicated by the high conductivity (4.87×10^{-3} S/cm) and the almost unity transference number (0.95). Song et al.³⁷ indicated that high crystallinity in polymers is unfavorable for ionic conductivity. When the polymer phase becomes amorphous, there is an increase of the disordered regions responsible for the ion conduction. There are no other structural changes upon heating the films to 150 °C, indicating the stability of the nanocomposites.

Acknowledgment. Support from BESSRC-CAT personnel at APS is greatly appreciated. Thanks to Roseann Csencsits of the Material Science Division, Argonne National Laboratory, for the TEM measurements. This work was performed under the auspices of the U.S. Department of Energy, Office of Basic Energy Sciences, Division of Chemical Sciences, Geosciences, and Biosciences under Contract No. W-31-109-ENG-38.

CM020670Z

(37) Song, J. Y.; Wang, Y. Y.; Wan, C. C. *J. Power Sources* **1999**, 77, 183.